

Supersymmetry contributions to CP violations in $b \rightarrow s$ and $b \rightarrow d$ transitions taking account of new data

Yusuke Shimizu,^{1,*} Morimitsu Tanimoto,^{1,†} and Kei Yamamoto^{2,‡}¹*Department of Physics, Niigata University, Niigata 950-2181, Japan*²*Graduate School of Science and Technology, Niigata University, Niigata 950-2181, Japan*

(Received 7 February 2013; published 8 March 2013)

We study the contribution of the gluino-squark mediated flavor changing process for the CP violation in $b \rightarrow s$ and $b \rightarrow d$ transitions taking account of recent experimental data. The mass insertion parameters of squarks are constrained by the branching ratios of $b \rightarrow s\gamma$ and $b \rightarrow d\gamma$ decays. In addition, the time-dependent CP asymmetries of $B^0 \rightarrow \phi K_S$ and $B^0 \rightarrow \eta' K^0$ decays severely restrict the allowed region of the mass insertion parameter for the $b \rightarrow s$ transition. By using these constraints with squark and gluino masses of 1.5 TeV, we predict the CP asymmetries of $B_s \rightarrow \phi\phi$, $B_s \rightarrow \eta'\phi$, and $B^0 \rightarrow K^0 \bar{K}^0$ decays, as well as the CP asymmetries in $b \rightarrow s\gamma$ and $b \rightarrow d\gamma$ decays. The CP violation in the $B_s \rightarrow \phi\phi$ decay is expected to be large owing to the squark flavor mixing, which will be tested at LHCb soon.

DOI: [10.1103/PhysRevD.87.056004](https://doi.org/10.1103/PhysRevD.87.056004)

PACS numbers: 11.30.Er, 12.60.Jv, 13.25.Hw

I. INTRODUCTION

The LHC experiments are now going on to discover new physics, for which supersymmetry (SUSY) is one of the most attractive candidates. SUSY signals have not yet been observed, although Higgs-like events are almost confirmed [1]. The lower bounds of the superparticle masses increase gradually. The squark and the gluino masses are expected to be larger than 1 TeV [2].

On the other hand, the LHCb Collaboration has reported new data of the CP violation of B mesons and the branching ratios of rare B decays [3–5]. The new physics is also expected to be indirectly found in the B meson decays. For many years, CP violation in the K and B^0 mesons has been successfully understood within the framework of the standard model (SM), the so-called Kobayashi-Maskawa model [6], where the source of the CP violation is the Kobayashi-Maskawa phase in the quark sector with three families, while there are new sources of CP violation if the SM is extended to the SUSY models. The soft squark mass matrices contain the CP -violating phases, which contribute to the flavor changing neutral current with the CP violation. Therefore, we expect the effect of the SUSY contribution in the CP -violating phenomena. However, clear deviation from the prediction of the SM has not been observed yet in the LHCb experiment [3–5].

In our previous works [7,8], we studied the SUSY contribution, which comes from the gluino-squark mediated flavor changing process [9–21]. We used the only experimental data of the $b \rightarrow s\gamma$ decay to constrain the mass insertion (MI) parameters of squarks. Then, we predicted the CP violations of a few $b \rightarrow s$ transition processes. In

the present paper, we give the systematic studies for the effect of the gluino-squark mediated flavor changing process in the CP violation of the $b \rightarrow s$ and $b \rightarrow d$ transitions. In order to obtain more precise numerical results, we take account of the QCD corrections for the SUSY contribution. Moreover, in order to constrain the MI parameters, we also input the recent experimental data, the time-dependent CP asymmetries of B^0 nonleptonic decays, in addition to the experimental data of the $b \rightarrow s\gamma$ decay.

The LHCb Collaboration reported the time-dependent CP asymmetry $S_{J/\psi\phi}$ in the nonleptonic B_s decay, which gives a constraint of the SUSY contribution on the $b \rightarrow s$ transition. The CP asymmetry of $B_s \rightarrow \phi\phi$ is expected to be observed in the near future at LHCb [5]. If there is a contribution of the squark flavor mixing in the flavor changing neutral current, we expect to observe the sizable time-dependent CP asymmetry in this process, in which the SM prediction is very small.

The typical process of the $b \rightarrow s$ transition is the $b \rightarrow s\gamma$ decay, in which the experimental data of the branching ratio, the direct CP violation, and the time-dependent CP asymmetry $S_{K^*\gamma}$ have been reported. The SUSY contribution is also constrained by the data of the time-dependent CP asymmetries in $B^0 \rightarrow \phi K_S$ and $B^0 \rightarrow \eta' K^0$ decays [22,23].

On the other hand, the $b \rightarrow d$ transition also becomes available to investigate the SUSY contribution quantitatively taking account of the recent experimental branching ratio of the $b \rightarrow d\gamma$ decay [24,25]. In this transition, the time-dependent CP asymmetry of the $B^0 \rightarrow K^0 \bar{K}^0$ decay is an attractive one to search for the SUSY effect, because the penguin amplitude dominates this process. We also predict the time-dependent CP asymmetry of $B^0 \rightarrow \rho\gamma$, $S_{\rho\gamma}$.

The dominant contribution of the SUSY is the gluino-squark mediated flavor changing process for

*shimizu@muse.sc.niigata-u.ac.jp

†tanimoto@muse.sc.niigata-u.ac.jp

‡yamamoto@muse.sc.niigata-u.ac.jp

the B meson decays discussed in this work. We present the constraint for the MI parameters $(\delta_d^{LR})_{23}$ and $(\delta_d^{LR})_{13}$ by putting the experimental data, where squarks and the gluino masses are at the TeV scale. By using these MI parameters, we predict the CP violation of the B meson decays, in which the interesting one is the $B_s \rightarrow \phi\phi$ decay. The CP violation in this decay will be measured at LHCb in the near future.

In Sec. II, we present the formulation of the gluino-squark contribution on the CP violation of B mesons in our framework. In Sec. III, we discuss the $b \rightarrow s$ transition and present numerical predictions for the direct CP violation and time-dependent CP asymmetries in $B^0 \rightarrow K^* \gamma$, $B_s \rightarrow \phi\phi$, and $B_s \rightarrow \eta' \phi$ decays. In Sec. IV, we discuss the $b \rightarrow d$ transition and present numerical predictions for the direct CP violation and time-dependent CP asymmetries in $B^0 \rightarrow \rho\gamma$ and $B^0 \rightarrow K^0 \bar{K}^0$ decays. Section V is devoted to the summary.

II. SQUARK FLAVOR MIXING IN CP VIOLATION OF B MESONS

Let us present the framework of the calculations for the contribution of the squark flavor mixing, which is the coupling among down-type quarks, down-type squarks, and the gluino. The effective Hamiltonian for the $\Delta B = 1$ process is given as

$$H_{\text{eff}} = \frac{4G_F}{\sqrt{2}} \left[\sum_{q'=u,c} V_{q'b} V_{q'q}^* \sum_{i=1,2} C_i O_i^{(q')} - V_{tb} V_{tq}^* \sum_{i=3-6,7\gamma,8G} (C_i O_i + \tilde{C}_i \tilde{O}_i) \right], \quad (1)$$

where $q = s, d$. The local operators are given as

$$\begin{aligned} O_1^{(q')} &= (\bar{q}_\alpha \gamma_\mu P_L q'_\beta) (\bar{q}'_\beta \gamma^\mu P_L b_\alpha), & O_2^{(q')} &= (\bar{q}_\alpha \gamma_\mu P_L q'_\alpha) (\bar{q}'_\beta \gamma^\mu P_L b_\beta), \\ O_3 &= (\bar{q}_\alpha \gamma_\mu P_L b_\alpha) \sum_Q (\bar{Q}_\beta \gamma^\mu P_L Q_\beta), & O_4 &= (\bar{q}_\alpha \gamma_\mu P_L b_\beta) \sum_Q (\bar{Q}_\beta \gamma^\mu P_L Q_\alpha), \\ O_5 &= (\bar{q}_\alpha \gamma_\mu P_L b_\alpha) \sum_Q (\bar{Q}_\beta \gamma^\mu P_R Q_\beta), & O_6 &= (\bar{q}_\alpha \gamma_\mu P_L b_\beta) \sum_Q (\bar{Q}_\beta \gamma^\mu P_R Q_\alpha), \\ O_{7\gamma} &= \frac{e}{16\pi^2} m_b \bar{q}_\alpha \sigma^{\mu\nu} P_R b_\alpha F_{\mu\nu}, & O_{8G} &= \frac{g_s}{16\pi^2} m_b \bar{q}_\alpha \sigma^{\mu\nu} P_R T_{\alpha\beta}^a b_\beta G_{\mu\nu}^a, \end{aligned} \quad (2)$$

where $P_R = (1 + \gamma_5)/2$, $P_L = (1 - \gamma_5)/2$, α and β are color indices, and Q is taken to be u, d, s, c quarks. Here, C_i 's and \tilde{C}_i 's are the Wilson coefficients, and \tilde{O}_i 's are the operators by replacing $L(R)$ with $R(L)$ in O_i . In this paper, C_i includes both the SM contribution and the gluino one, such as $C_i = C_i^{\text{SM}} + C_i^{\tilde{g}}$, where C_i^{SM} 's are given in Ref. [26].

In order to estimate the SUSY contribution for $C_i^{\tilde{g}}$, we take the most popular ansatz, a degenerate SUSY breaking mass spectrum for the flavor structure of squarks. In the super-Cabibbo-Kobayashi-Maskawa basis, we can parametrize the soft scalar masses squared of the down-type squarks, $M_{d_{LL}}^2$, $M_{d_{RR}}^2$, $M_{d_{LR}}^2$, and $M_{d_{RL}}^2$, as follows:

$$\begin{aligned} M_{d_{LL}}^2 &= m_{\tilde{q}}^2 \begin{pmatrix} 1 + (\delta_d^{LL})_{11} & (\delta_d^{LL})_{12} & (\delta_d^{LL})_{13} \\ (\delta_d^{LL})_{12}^* & 1 + (\delta_d^{LL})_{22} & (\delta_d^{LL})_{23} \\ (\delta_d^{LL})_{13}^* & (\delta_d^{LL})_{23}^* & 1 + (\delta_d^{LL})_{33} \end{pmatrix}, \\ M_{d_{RR}}^2 &= m_{\tilde{q}}^2 \begin{pmatrix} 1 + (\delta_d^{RR})_{11} & (\delta_d^{RR})_{12} & (\delta_d^{RR})_{13} \\ (\delta_d^{RR})_{12}^* & 1 + (\delta_d^{RR})_{22} & (\delta_d^{RR})_{23} \\ (\delta_d^{RR})_{13}^* & (\delta_d^{RR})_{23}^* & 1 + (\delta_d^{RR})_{33} \end{pmatrix}, \\ M_{d_{LR}}^2 &= (M_{d_{RL}}^2)^\dagger = m_{\tilde{q}}^2 \begin{pmatrix} (\delta_d^{LR})_{11} & (\delta_d^{LR})_{12} & (\delta_d^{LR})_{13} \\ (\delta_d^{LR})_{21} & (\delta_d^{LR})_{22} & (\delta_d^{LR})_{23} \\ (\delta_d^{LR})_{31} & (\delta_d^{LR})_{32} & (\delta_d^{LR})_{33} \end{pmatrix}, \end{aligned} \quad (3)$$

where $m_{\tilde{q}}$ is the average squark mass and $(\delta_d^{LL})_{ij}$, $(\delta_d^{RR})_{ij}$, $(\delta_d^{LR})_{ij}$, and $(\delta_d^{RL})_{ij}$ are called MI parameters.

The Wilson coefficients of the gluino contribution $C_i^{\tilde{g}}$ are given as follows [27]:

$$\begin{aligned}
 C_3^{\bar{g}}(m_{\bar{g}}) &\simeq \frac{\sqrt{2}\alpha_s^2}{4G_F V_{ib} V_{iq}^* m_{\bar{q}}^2} (\delta_d^{LL})_{k3} \left[-\frac{1}{9} B_1(x) - \frac{5}{9} B_2(x) - \frac{1}{18} P_1(x) - \frac{1}{2} P_2(x) \right], \\
 C_4^{\bar{g}}(m_{\bar{g}}) &\simeq \frac{\sqrt{2}\alpha_s^2}{4G_F V_{ib} V_{iq}^* m_{\bar{q}}^2} (\delta_d^{LL})_{k3} \left[-\frac{7}{3} B_1(x) + \frac{1}{3} B_2(x) + \frac{1}{6} P_1(x) + \frac{3}{2} P_2(x) \right], \\
 C_5^{\bar{g}}(m_{\bar{g}}) &\simeq \frac{\sqrt{2}\alpha_s^2}{4G_F V_{ib} V_{iq}^* m_{\bar{q}}^2} (\delta_d^{LL})_{k3} \left[\frac{10}{9} B_1(x) + \frac{1}{18} B_2(x) - \frac{1}{18} P_1(x) - \frac{1}{2} P_2(x) \right], \\
 C_6^{\bar{g}}(m_{\bar{g}}) &\simeq \frac{\sqrt{2}\alpha_s^2}{4G_F V_{ib} V_{iq}^* m_{\bar{q}}^2} (\delta_d^{LL})_{k3} \left[-\frac{2}{3} B_1(x) + \frac{7}{6} B_2(x) + \frac{1}{6} P_1(x) + \frac{3}{2} P_2(x) \right], \\
 C_{7\gamma}^{\bar{g}}(m_{\bar{g}}) &\simeq -\frac{\sqrt{2}\alpha_s \pi}{6G_F V_{ib} V_{iq}^* m_{\bar{q}}^2} \left[(\delta_d^{LL})_{k3} \left(\frac{8}{3} M_3(x) - \mu \tan \beta \frac{m_{\bar{g}}}{m_{\bar{q}}^2} \frac{8}{3} M_a(x) \right) + (\delta_d^{LR})_{k3} \frac{m_{\bar{g}}}{m_b} \frac{8}{3} M_1(x) \right], \\
 C_{8G}^{\bar{g}}(m_{\bar{g}}) &\simeq -\frac{\sqrt{2}\alpha_s \pi}{2G_F V_{ib} V_{iq}^* m_{\bar{q}}^2} \left[(\delta_d^{LL})_{k3} \left\{ \left(\frac{1}{3} M_3(x) + 3M_4(x) \right) - \mu \tan \beta \frac{m_{\bar{g}}}{m_{\bar{q}}^2} \left(\frac{1}{3} M_a(x) + 3M_b(x) \right) \right\} \right. \\
 &\quad \left. + (\delta_d^{LR})_{k3} \frac{m_{\bar{g}}}{m_b} \left(\frac{1}{3} M_1(x) + 3M_2(x) \right) \right], \tag{4}
 \end{aligned}$$

where $k = 2, 1$ correspond to $b \rightarrow q$ ($q = s, d$) transitions, respectively. Here the double mass insertion is included in $C_{7\gamma}^{\bar{g}}(m_{\bar{g}})$ and $C_{8G}^{\bar{g}}(m_{\bar{g}})$. The Wilson coefficients $\tilde{C}_i^{\bar{g}}(m_{\bar{g}})$'s are obtained by replacing $L(R)$ with $R(L)$ in $C_i^{\bar{g}}(m_{\bar{g}})$'s. The loop functions in Eq. (4) are presented in our previous work [7]. In our calculations, $C_{7\gamma}$ and C_{8G} give dominant contributions to the CP violations in $b \rightarrow s$ and $b \rightarrow d$ transitions. The effective Wilson coefficients of $C_{7\gamma}(m_b)$ and $C_{8G}(m_b)$ are given at the leading order of QCD as follows [26]:

$$C_{7\gamma}^{\bar{g}}(m_b) = \zeta C_{7\gamma}^{\bar{g}}(m_{\bar{g}}) + \frac{8}{3} (\eta - \zeta) C_{8G}^{\bar{g}}(m_{\bar{g}}), \tag{5}$$

$$C_{8G}^{\bar{g}}(m_b) = \eta C_{8G}^{\bar{g}}(m_{\bar{g}}),$$

where

$$\begin{aligned}
 \zeta &= \left(\frac{\alpha_s(m_{\bar{g}})}{\alpha_s(m_t)} \right)^{\frac{16}{21}} \left(\frac{\alpha_s(m_t)}{\alpha_s(m_b)} \right)^{\frac{16}{23}}, \\
 \eta &= \left(\frac{\alpha_s(m_{\bar{g}})}{\alpha_s(m_t)} \right)^{\frac{14}{21}} \left(\frac{\alpha_s(m_t)}{\alpha_s(m_b)} \right)^{\frac{14}{23}}.
 \end{aligned} \tag{6}$$

Let us discuss the time-dependent CP asymmetries of B^0 and B_s decaying into the final state f , which are defined as [28]

$$S_f = \frac{2 \text{Im} \lambda_f}{1 + |\lambda_f|^2}, \quad C_f = \frac{1 - |\lambda_f|^2}{1 + |\lambda_f|^2}, \tag{7}$$

where

$$\lambda_f = \frac{q}{p} \bar{\rho}, \quad \frac{q}{p} \simeq \sqrt{\frac{M_{12}^{q*}}{M_{12}^q}}, \quad \bar{\rho} \equiv \frac{\bar{A}(\bar{B}_q^0 \rightarrow f)}{A(B_q^0 \rightarrow f)}. \tag{8}$$

Here M_{12}^q ($q = s, d$) are the dispersive parts of the B_q - \bar{B}_q mixing, in which the quark-squark-gluino interaction contributes in addition to the SM one. The MI parameters $(\delta_d^{LL})_{k3}$ and $(\delta_d^{RR})_{k3}$ ($k = 2, 1$) are constrained by CP violations in the

$\Delta B = 2$ transition as discussed in our previous works [7,8]. On the other hand, $(\delta_d^{LR})_{k3}$ and $(\delta_d^{RL})_{k3}$ ($k = 2, 1$) are constrained in the $\Delta B = 1$ transition.

In the $B^0 \rightarrow J/\psi K_S$ and $B_s \rightarrow J/\psi \phi$ decays, we write $\lambda_{J/\psi K_S}$ and $\lambda_{J/\psi \phi}$ in terms of phase factors, respectively:

$$\lambda_{J/\psi K_S} \equiv -e^{-i\phi_d}, \quad \lambda_{J/\psi \phi} \equiv e^{-i\phi_s}. \tag{9}$$

The recent experimental data of these phases are [23,29]

$$\begin{aligned}
 \sin \phi_d &= 0.679 \pm 0.020, \\
 \phi_s &= -0.002 \pm 0.083 \pm 0.027.
 \end{aligned} \tag{10}$$

We expect the SUSY contribution to be included in these observed values.

Since the $B^0 \rightarrow J/\psi K_S$ process occurs at the tree level in the SM, the CP asymmetry mainly originates from M_{12}^d . Although the $B^0 \rightarrow \phi K_S$ and $B^0 \rightarrow \eta' K^0$ decays are penguin dominant ones, their CP asymmetries also come from M_{12}^d in the SM. Then, the CP asymmetries of $B^0 \rightarrow J/\psi K_S$, $B^0 \rightarrow \phi K_S$, and $B^0 \rightarrow \eta' K^0$ decays are expected to be the same magnitude.

On the other hand, if the squark flavor mixing contributes to the decay at the one-loop level, its magnitude could be comparable to the SM penguin one in $B^0 \rightarrow \phi K_S$ and $B^0 \rightarrow \eta' K^0$ decays, but the squark flavor mixing contribution is tiny in the $B^0 \rightarrow J/\psi K_S$ decay, because this process is at the tree level in the SM. Therefore, there is a possibility to find the SUSY contribution by observing the different CP asymmetries among those processes [30].

The time-dependent CP asymmetry $S_{J/\psi K_S}$ has been precisely measured. On the other hand, Particle Data Group [22] and the Heavy Flavor Averaging Group (HFAG) [23] presented considerably different values for $S_{\phi K_S}$ while almost the same one for $S_{\eta' K^0}$. Each of the observed ones in HFAG is consistent with the SM

prediction. In order to get conservative constraints, we take the data of these time-dependent CP asymmetries in HFAG [23], which are

$$S_{J/\psi K_S} = 0.679 \pm 0.020, \quad S_{\phi K_S} = 0.74_{-0.13}^{+0.11},$$

$$S_{\eta' K^0} = 0.59 \pm 0.07. \quad (11)$$

These values may be regarded to be the same within the experimental error bar. Thus, the experimental values are consistent with the prediction of the SM. In other words, these data severely constrain the MI parameters $(\delta_d^{LR})_{23}$ and $(\delta_d^{RL})_{23}$ in our following analyses.

III. THE $b \rightarrow s$ TRANSITION

At first, we discuss the contributions of the squark flavor mixing for the $b \rightarrow s$ transition, which are given in terms of the MI parameters $(\delta_d^{LL})_{23}$, $(\delta_d^{RR})_{23}$, $(\delta_d^{LR})_{23}$, and $(\delta_d^{RL})_{23}$. These MI parameters are constrained by the experimental data of B meson decays.

Let us show the formulation of the $b \rightarrow s$ transition. The CP asymmetries S_f of Eq. (7) in the $b \rightarrow s\bar{s}$ transition are one of the most important processes when we investigate the new physics. The CP asymmetries S_f for $B^0 \rightarrow \phi K_S$ and $B^0 \rightarrow \eta' K^0$ are given in terms of λ_f in Eq. (8):

$$\lambda_{\phi K_S, \eta' K^0} = -e^{-i\phi_d} \frac{\sum_{i=3-6,7\gamma,8G} (C_i^{\text{SM}} \langle O_i \rangle + C_i^{\tilde{g}} \langle O_i \rangle + \tilde{C}_i^{\tilde{g}} \langle \tilde{O}_i \rangle)}{\sum_{i=3-6,7\gamma,8G} (C_i^{\text{SM}*} \langle O_i \rangle + C_i^{\tilde{g}*} \langle O_i \rangle + \tilde{C}_i^{\tilde{g}*} \langle \tilde{O}_i \rangle)}, \quad (12)$$

where $\langle O_i \rangle$ is the abbreviation of $\langle f | O_i | B^0 \rangle$. It is noticed that $\langle \phi K_S | O_i | B^0 \rangle = \langle \phi K_S | \tilde{O}_i | B^0 \rangle$ and $\langle \eta' K^0 | O_i | B^0 \rangle = -\langle \eta' K^0 | \tilde{O}_i | B^0 \rangle$, because these final states have different parities [30,31]. Since the dominant term comes from the gluon penguin $C_{8G}^{\tilde{g}}$, the decay amplitudes of $f = \phi K_S$ and $f = \eta' K^0$ are given as follows:

$$\bar{A}(\bar{B}^0 \rightarrow \phi K_S) \propto C_{8G}(m_b) + \tilde{C}_{8G}(m_b),$$

$$\bar{A}(\bar{B}^0 \rightarrow \eta' \bar{K}^0) \propto C_{8G}(m_b) - \tilde{C}_{8G}(m_b). \quad (13)$$

Since $\tilde{C}_{8G}(m_b)$ is suppressed compared to $C_{8G}(m_b)$ in the SM, the magnitudes of the time-dependent CP asymmetries S_f ($f = J/\psi \phi$, ϕK_S , $\eta' K^0$) are almost the same in the SM prediction. However, the squark flavor mixing gives the unsuppressed $\tilde{C}_{8G}(m_b)$; then, the CP asymmetries in those decays are expected to be deviated among them. Therefore, those experimental data give us the tight constraint for $C_{8G}(m_b)$ and $\tilde{C}_{8G}(m_b)$.

We have also λ_f for $B_s \rightarrow \phi \phi$ and $B_s \rightarrow \phi \eta'$ as follows:

$$\lambda_{\phi \phi, \phi \eta'} = e^{-i\phi_s} \frac{\sum_{i=3-6,7\gamma,8G} (C_i^{\text{SM}} \langle O_i \rangle + C_i^{\tilde{g}} \langle O_i \rangle + \tilde{C}_i^{\tilde{g}} \langle \tilde{O}_i \rangle)}{\sum_{i=3-6,7\gamma,8G} (C_i^{\text{SM}*} \langle O_i \rangle + C_i^{\tilde{g}*} \langle O_i \rangle + \tilde{C}_i^{\tilde{g}*} \langle \tilde{O}_i \rangle)}, \quad (14)$$

with $\langle \phi \phi | O_i | B_s \rangle = -\langle \phi \phi | \tilde{O}_i | B_s \rangle$ and $\langle \phi \eta' | O_i | B_s \rangle = \langle \phi \eta' | \tilde{O}_i | B_s \rangle$. The decay amplitudes of $f = \phi \phi$ and $f = \phi \eta'$ are given as follows:

$$\bar{A}(\bar{B}_s \rightarrow \phi \phi) \propto C_{8G}(m_b) - \tilde{C}_{8G}(m_b),$$

$$\bar{A}(\bar{B}_s \rightarrow \phi \eta') \propto C_{8G}(m_b) + \tilde{C}_{8G}(m_b). \quad (15)$$

Since $C_{8G} \langle O_{8G} \rangle$ and $\tilde{C}_{8G} \langle \tilde{O}_{8G} \rangle$ dominate these amplitudes, our numerical results are insensitive to the hadronic matrix elements. In order to obtain precise results, we also take account of the small contributions from other Wilson coefficients C_i ($i = 3, 4, 5, 6$) and \tilde{C}_i ($i = 3, 4, 5, 6$) in our calculations. We estimate each hadronic matrix element by using the factorization relations in Ref. [32]:

$$\langle O_3 \rangle = \langle O_4 \rangle = \left(1 + \frac{1}{N_c}\right) \langle O_5 \rangle, \quad \langle O_6 \rangle = \frac{1}{N_c} \langle O_5 \rangle,$$

$$\langle O_{8G} \rangle = \frac{\alpha_s(m_b)}{8\pi} \left(-\frac{2m_b}{\sqrt{\langle q^2 \rangle}}\right)$$

$$\times \left(\langle O_4 \rangle + \langle O_6 \rangle - \frac{1}{N_c} (\langle O_3 \rangle + \langle O_5 \rangle)\right), \quad (16)$$

where $\langle q^2 \rangle = 6.3 \text{ GeV}^2$ and $N_c = 3$ is the number of colors. One may worry about the reliability of these naive factorization relations. However, this approximation has been justified numerically in the relevant $b \rightarrow s$ transition as seen in the calculation of perturbative QCD [33].

Let us discuss the contribution of the MI parameters to $C_{8G}^{\tilde{g}}$ in Eq. (4). Since the loop functions are of the same order and $m_{\tilde{q}} \simeq m_{\tilde{g}}$, the ratio of the LL component and the LR one is $(\delta_d^{LL})_{23} \times \mu \tan \beta / m_{\tilde{q}}$ to $(\delta_d^{LR})_{23} \times m_{\tilde{q}} / m_b$. If $\mathcal{O}(\mu \tan \beta) \simeq \mathcal{O}(m_{\tilde{q}})$ and $m_{\tilde{q}} \gtrsim 1 \text{ TeV}$, the LR component may contribute significantly to $C_{8G}^{\tilde{g}}$ due to the enhancement factor $m_{\tilde{q}} / m_b = \mathcal{O}(10^2)$. For example, in the case of $(\delta_d^{LL})_{23} = 10^{-2}$ and $(\delta_d^{LR})_{23} = 10^{-3}$, the LR component dominates $C_{8G}^{\tilde{g}}$, while it is minor in M_{12}^d [7,8]. Actually, the magnitude of $(\delta_d^{LL})_{23}$ is at most 10^{-2} , which was estimated in our previous works [7,8]. In our following calculations, we take $|(\delta_d^{LL})_{23}| \lesssim 10^{-2}$.

We can also constrain the SUSY contribution from the $b \rightarrow s\gamma$ decay. Here we discuss three observable values; those are the branching ratio $\text{BR}(b \rightarrow s\gamma)$, the direct CP asymmetry $A_{CP}^{b \rightarrow s\gamma}$, and the time-dependent CP asymmetry

of $B^0 \rightarrow K^* \gamma$, $S_{K^* \gamma}$. The branching ratio $\text{BR}(b \rightarrow q \gamma)$ ($q = s, d$) is a typical process to investigate the new physics. It is given as [34]

$$\frac{\text{BR}(b \rightarrow q \gamma)}{\text{BR}(b \rightarrow ce \bar{\nu}_e)} = \frac{|V_{tq}^* V_{tb}|^2}{|V_{cb}|^2} \frac{6\alpha}{\pi f(z)} (|C_{7\gamma}(m_b)|^2 + |\tilde{C}_{7\gamma}(m_b)|^2), \quad (17)$$

where

$$f(z) = 1 - 8z + 8z^3 - z^4 - 12z^2 \ln z, \quad z = \frac{m_{c,\text{pole}}^2}{m_{b,\text{pole}}^2}. \quad (18)$$

Here $C_{7\gamma}(m_b)$ and $\tilde{C}_{7\gamma}(m_b)$ include both contributions from the SM and the gluino-squark mediated flavor changing process at the m_b scale. As seen in Eq. (4), MI parameters $(\delta_d^{LR})_{k3}$ dominate both $C_{7\gamma}^{\tilde{g}}$ and $C_{8G}^{\tilde{g}}$. Therefore, we should discuss the contribution from $(\delta_d^{LR})_{k3}$ in our numerical calculations.

We can also estimate the direct CP violation $A_{CP}^{b \rightarrow q \gamma}$ in the $b \rightarrow q \gamma$ decay ($q = s, d$), which is given as [35]

$$\begin{aligned} A_{CP}^{b \rightarrow q \gamma} &= \frac{\Gamma(\bar{B} \rightarrow X_q \gamma) - \Gamma(B \rightarrow X_{\bar{q}} \gamma)}{\Gamma(\bar{B} \rightarrow X_q \gamma) + \Gamma(B \rightarrow X_{\bar{q}} \gamma)} \Big|_{E_{\gamma} > (1-\delta)E_{\gamma}^{\text{max}}} \\ &= \frac{\alpha_s(m_b)}{|C_{7\gamma}|^2 + |\tilde{C}_{7\gamma}|^2} \left[\frac{40}{81} \text{Im}[C_2 C_{7\gamma}^*] - \frac{8z}{9} [v(z) \right. \\ &\quad \left. + b(z, \delta)] \text{Im} \left[\left(1 + \frac{V_{uq}^* V_{ub}}{V_{tq}^* V_{tb}} \right) C_2 C_{7\gamma}^* \right] \right. \\ &\quad \left. - \frac{4}{9} \text{Im}[C_{8G} C_{7\gamma}^* + \tilde{C}_{8G} \tilde{C}_{7\gamma}^*] \right. \\ &\quad \left. + \frac{8z}{27} b(z, \delta) \text{Im} \left[\left(1 + \frac{V_{uq}^* V_{ub}}{V_{tq}^* V_{tb}} \right) C_2 C_{8G}^* \right] \right], \quad (19) \end{aligned}$$

where $v(z)$ and $b(z, \delta)$ are explicitly given in Ref. [35] and C_i and \tilde{C}_i ($i = 7\gamma, 8G$) include both the SM and SUSY contributions at the m_b scale.

The time-dependent CP asymmetry $S_{K^* \gamma}$ in the $B^0 \rightarrow K^* \gamma$ decay is also an important measure of the CP violation:

$$S_{K^* \gamma} = \frac{2 \text{Im}(-e^{-i\phi_d} \tilde{C}_{7\gamma}(m_b)/C_{7\gamma}(m_b))}{|\tilde{C}_{7\gamma}(m_b)/C_{7\gamma}(m_b)|^2 + 1}. \quad (20)$$

This CP violation comes from the interference between $C_{7\gamma}(m_b)$ and $\tilde{C}_{7\gamma}(m_b)$ [27,36]. In the SM, $\tilde{C}_{7\gamma}^{\text{SM}}(m_b)/C_{7\gamma}^{\text{SM}}(m_b) \propto m_s/m_b$ for this process. Therefore, $S_{K^* \gamma}$ is suppressed [36]. However, $S_{K^* \gamma}$ could be enhanced owing to the squark flavor mixing.

Our setup in our calculations is shown as follows. We take $\mu \tan \beta$ to be 1 TeV and set $|(\delta_d^{LR})_{23}| \simeq |(\delta_d^{RR})_{23}| \lesssim 10^{-2}$ following from our previous works [7,8]. Then, the

contribution of these MI parameters to $C_{7\gamma}^{\tilde{g}}$ and $C_{8G}^{\tilde{g}}$ are minor. On the other hand, $(\delta_d^{LR})_{23}$ and $(\delta_d^{RL})_{23}$ are severely constrained by magnitudes of $C_{7\gamma}$ and C_{8G} . In addition, we suppose $|(\delta_d^{LR})_{23}| = |(\delta_d^{RL})_{23}|$. Then, we can parametrize the MI parameters as follows:

$$(\delta_d^{LR})_{23} = |(\delta_d^{LR})_{23}| e^{2i\theta_{23}^{LR}}, \quad (\delta_d^{RL})_{23} = |(\delta_d^{LR})_{23}| e^{2i\theta_{23}^{RL}}. \quad (21)$$

Now we show numerical analysis in our setup. In our following numerical calculations, we fix the squark mass and the gluino mass as

$$m_{\tilde{q}} = 1.5 \text{ TeV}, \quad m_{\tilde{g}} = 1.5 \text{ TeV}, \quad (22)$$

which are consistent with the recent lower bound of these masses at LHC [2].

In our analysis, the present experimental data of $\text{BR}(b \rightarrow s \gamma)$, $S_{J/\psi K_S}$, $S_{\phi K_S}$, and $S_{\eta' K^0}$ give tight constraints for MI parameters. Here we put the experimental data [22]

$$\text{BR}(b \rightarrow s \gamma)(\text{exp}) = (3.53 \pm 0.24) \times 10^{-4}; \quad (23)$$

on the other hand, the SM has predicted [37]

$$\text{BR}(b \rightarrow s \gamma)(\text{SM}) = (3.15 \pm 0.23) \times 10^{-4}. \quad (24)$$

Therefore, there is room for the contribution of the gluino-squark mediated flavor changing process.¹ For $S_{J/\psi K_S}$, $S_{\phi K_S}$, and $S_{\eta' K^0}$, we put the data in Eq. (11). In the SM, these magnitudes of S_f agree among them.

At first, in Fig. 1(a), we show the allowed region in the plane of the absolute value $|(\delta_d^{LR})_{23}|$ and the phase θ_{23}^{LR} , where the only experimental constraint of $\text{BR}(b \rightarrow s \gamma)$ is put. The magnitude of the MI parameter $(\delta_d^{LR})_{23}$ is allowed as $|(\delta_d^{LR})_{23}| \lesssim 9 \times 10^{-2}$. We note that the SUSY contribution to $\text{BR}(b \rightarrow s \gamma)$ becomes superior compared with the SM in the region of $|(\delta_d^{LR})_{23}| \gtrsim 4 \times 10^{-2}$. It is also noted that the $(\delta_d^{LR})_{23}$ is almost real around the upper bound 9×10^{-2} , that is, at $2\theta_{23}^{LR} = 0$ or 2π . The experimental constraints of $S_{J/\psi K_S}$, $S_{\phi K_S}$, and $S_{\eta' K^0}$ give the severe cut as seen in Fig. 1(b), where these experimental data are put in addition to $\text{BR}(b \rightarrow s \gamma)$. In this figure, any value of the phase is allowed in $|(\delta_d^{LR})_{23}| \lesssim 5 \times 10^{-3}$. On the other hand, the larger region of $|(\delta_d^{LR})_{23}|$ is allowed until 2×10^{-2} around the specific θ_{23}^{LR} , $\pi/4$, and $3\pi/4$.² The obtained bound $|(\delta_d^{LR})_{23}| \lesssim 2 \times 10^{-2}$ depends on the gluino and the squark masses. If they

¹In our analysis, we do not take account of the contribution of the charged Higgs and chargino in $b \rightarrow s \gamma$.

²There still remains a very small allowed region around $|(\delta_d^{LR})_{23}| = 9 \times 10^{-2}$, where $(\delta_d^{LR})_{23}$ is almost real, since this region cannot be excluded by the time-dependent CP asymmetries. In our work, we omit this region hereafter. This region is uninteresting, because the SUSY contribution is much larger than the SM one in $b \rightarrow s \gamma$.

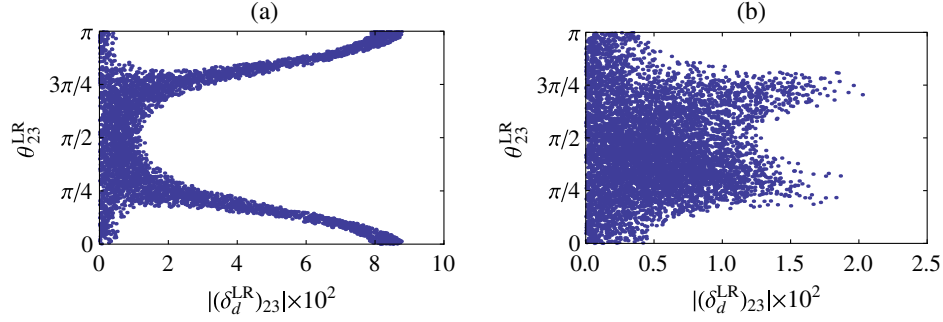


FIG. 1 (color online). The predicted region of $(\delta_d^{LR})_{23}$. In both (a) and (b), the horizontal and vertical axes denote the absolute value and the phase of $(\delta_d^{LR})_{23}$, respectively. In (a), the only experimental constraint of $\text{BR}(b \rightarrow s\gamma)$ is taken into account. In (b), the experimental constraints of $\text{BR}(b \rightarrow s\gamma)$, $S_{\phi_{K_S}}$, and $S_{\eta'K^0}$ are taken into account.

increase, the upper bound is rescaled approximately as $|(\delta_d^{LR})_{23}| \times m_{\bar{q}}/(1.5 \text{ TeV})$.

By using this allowed region of $(\delta_d^{LR})_{23}$, we predict $A_{CP}^{b \rightarrow s\gamma}$, $S_{K^*\gamma}$, S_{ϕ_ϕ} , and $S_{\phi_{\eta'}}$. In Fig. 2, we show the predicted direct CP asymmetry $A_{CP}^{b \rightarrow s\gamma}$ versus $|(\delta_d^{LR})_{23}|$. Here the value at $|(\delta_d^{LR})_{23}| = 0$ is the SM one, $A_{CP}^{b \rightarrow s\gamma}(\text{SM}) \simeq 4 \times 10^{-3}$ [35]. We predict $-3 \times 10^{-2} \lesssim A_{CP}^{b \rightarrow s\gamma} \lesssim 3 \times 10^{-2}$ owing to the squark flavor mixing. Recent experimental data are still consistent with our prediction due to the large error as seen in $A_{CP}^{b \rightarrow s\gamma}(\text{exp}) = -0.008 \pm 0.029$ [22]. The precise data will give us an additional constraint of the MI parameters in the future.

In Fig. 3, we show the predicted CP asymmetry $S_{K^*\gamma}$. The predicted value in the SM is $S_{K^*\gamma}(\text{SM}) \simeq (2m_s/m_b) \sin \phi_d \simeq 4 \times 10^{-2}$ [36], while the experimental result is $S_{K^*\gamma}(\text{exp}) = -0.15 \pm 0.22$ [22]. Our prediction is $-0.4 \lesssim S_{K^*\gamma} \lesssim 0.2$, which is still consistent with the experimental data. We also expect the precise data in the near future to test our prediction.

Although the experimental data of the time-dependent CP asymmetries $S_{\phi_{K_S}}$ and $S_{\eta'K^0}$ are taken as the input

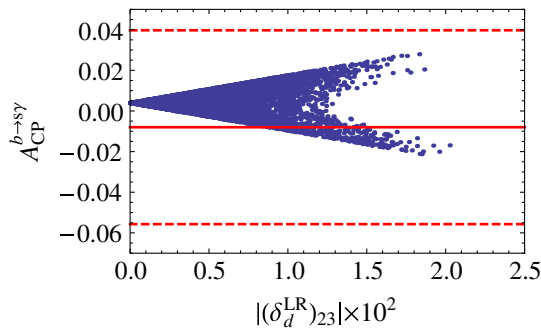


FIG. 2 (color online). The predicted direct CP asymmetry $A_{CP}^{b \rightarrow s\gamma}$ of $b \rightarrow s\gamma$ versus $|(\delta_d^{LR})_{23}|$. The red solid and two red dotted lines denote the best fit value and upper and lower bounds of the experimental data with 90% C.L., respectively.

in our analysis, these calculated values do not always cover all experimental allowed regions due to the constraint from $\text{BR}(b \rightarrow s\gamma)$. Those allowed regions are shown in Fig. 4. The SM prediction is $S_{J/\psi K_S}(\text{SM}) = S_{\phi_{K_S}}(\text{SM}) = S_{\eta'K^0}(\text{SM})$, while the present data of these

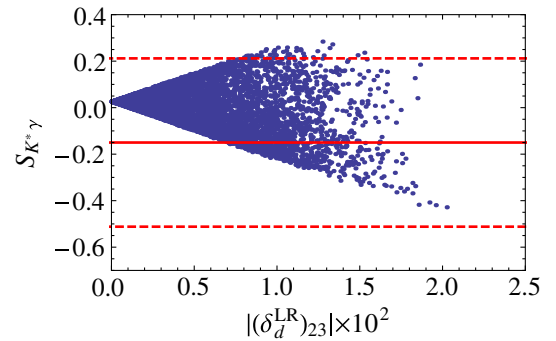


FIG. 3 (color online). The predicted CP asymmetry $S_{K^*\gamma}$ of $B^0 \rightarrow K^*\gamma$ versus $|(\delta_d^{LR})_{23}|$, where the red solid and two red dotted lines denote the best fit value and upper and lower bounds of the experimental data with 90% C.L., respectively.

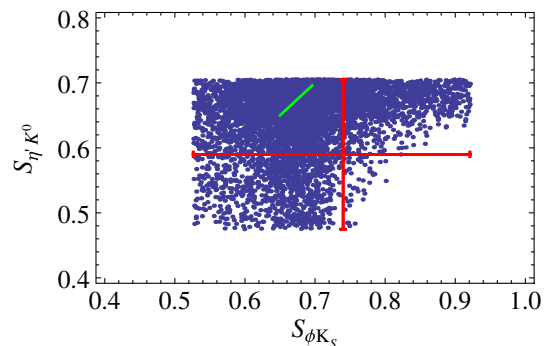


FIG. 4 (color online). The allowed region of the time-dependent CP asymmetries on the $S_{\phi_{K_S}} - S_{\eta'K^0}$ plane. The SM prediction $S_{J/\psi K_S} = S_{\phi_{K_S}} = S_{\eta'K^0}$ is plotted by the green slanted line. The experimental data with error bar is plotted by the red solid lines at 90% C.L.

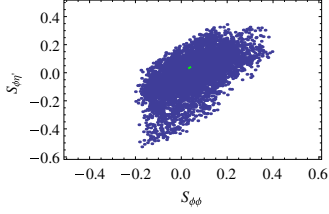


FIG. 5 (color online). The predicted time-dependent CP asymmetries on the $S_{\phi\phi}$ - $S_{\phi\eta'}$ plane. The small green line denotes the SM prediction from the experimental data of $S_{J/\psi\phi}$.

time-dependent CP asymmetries are given in Eq. (11). The region of the lower right corner in the figure is excluded. It will be testable in future experiments.

In Fig. 5, we predict the time-dependent CP asymmetries $S_{\phi\phi}$ and $S_{\phi\eta'}$. These CP asymmetries must be equal to $S_{J/\psi\phi}$ in the SM. We use the experimental result of $S_{J/\psi\phi}$ for the phase ϕ_s , which is given in Eq. (10), in our calculations. We denote the small green line as the SM value $S_{J/\psi\phi}(\text{SM}) = 0.0363^{+0.0016}_{-0.0015}$ [38] in the figure. In conclusion, we predict $-0.2 \lesssim S_{\phi\phi} \lesssim 0.4$ and $-0.5 \lesssim S_{\phi\eta'} \lesssim 0.4$, respectively. Since the phase ϕ_s has still a large experimental error bar, our prediction will be improved if the precise experimental data of $S_{J/\psi\phi}$ are given in the near future at LHCb. Since the time-dependent CP asymmetry $S_{\phi\phi}$ will be measured at LHCb, our prediction will be tested soon.

IV. THE $b \rightarrow d$ TRANSITION

In this section, we discuss the $b \rightarrow d$ transition in the same way as the $b \rightarrow s$ one. The SUSY contribution is given in terms of the MI parameters $(\delta_d^{LL})_{13}$, $(\delta_d^{RR})_{13}$, $(\delta_d^{LR})_{13}$, and $(\delta_d^{RL})_{13}$. The typical $b \rightarrow d$ transition is the $b \rightarrow d\gamma$ decay. The experimental data of its branching ratio give the constraint for these MI parameters. By using these MI parameters, we calculate SUSY contributions to the direct CP violation of the $b \rightarrow d\gamma$ decay and the time-dependent CP asymmetry in the $B^0 \rightarrow \rho\gamma$ decay. We also predict the time-dependent CP asymmetry of the $B^0 \rightarrow K^0\bar{K}^0$ decay.

In order to constrain the MI parameters, we input the experimental data of the branching ratio of $b \rightarrow d\gamma$ [24,25],

$$\text{BR}(b \rightarrow d\gamma)(\text{exp}) = (1.41 \pm 0.57) \times 10^{-5}; \quad (25)$$

on the other hand, the SM has predicted [25]

$$\text{BR}(b \rightarrow d\gamma)(\text{SM}) = (1.54^{+0.26}_{-0.31}) \times 10^{-5}. \quad (26)$$

Next we present the formulations of the time-dependent CP asymmetries and direct CP violation including SUSY contributions. The branching ratio and direct CP violation in the $b \rightarrow d\gamma$ decay are given in Eqs. (17) and (19), respectively. The time-dependent CP asymmetry $S_{\rho\gamma}$ in

the $B^0 \rightarrow \rho\gamma$ decay is an important observable to search for the new physics and is given as

$$S_{\rho\gamma} = \frac{2 \text{Im}(-e^{-i\phi_d} \tilde{C}_{7\gamma}(m_b)/C_{7\gamma}(m_b))}{|\tilde{C}_{7\gamma}(m_b)/C_{7\gamma}(m_b)|^2 + 1}. \quad (27)$$

Since $\tilde{C}_{7\gamma}^{\text{SM}}(m_b)/C_{7\gamma}^{\text{SM}}(m_b) \propto m_d/m_b$ in the SM, $S_{\rho\gamma}$ may be expected to be quite suppressed [36]. However, $S_{\rho\gamma}$ could be also enhanced owing to the gluino-squark mediated flavor changing process.

The time-dependent CP asymmetries $S_{K^0\bar{K}^0}$ and $C_{K^0\bar{K}^0}$ in the $B^0 \rightarrow K^0\bar{K}^0$ decay are also interesting ones to search for the new physics, since there is no tree process of the SM in the $B^0 \rightarrow K^0\bar{K}^0$ decay [39,40]. These CP asymmetries are given in Eq. (7) as

$$S_{K^0\bar{K}^0} = \frac{2 \text{Im}\lambda_{K^0\bar{K}^0}}{1 + |\lambda_{K^0\bar{K}^0}|^2}, \quad C_{K^0\bar{K}^0} = \frac{1 - |\lambda_{K^0\bar{K}^0}|^2}{1 + |\lambda_{K^0\bar{K}^0}|^2}, \quad (28)$$

where

$$\lambda_{K^0\bar{K}^0} = \frac{q}{p} \bar{\rho}, \quad \frac{q}{p} \simeq \sqrt{\frac{M_{12}^{d*}}{M_{12}^d}}, \quad \bar{\rho} \equiv \frac{\bar{A}(\bar{B}^0 \rightarrow K^0\bar{K}^0)}{A(B^0 \rightarrow K^0\bar{K}^0)}. \quad (29)$$

The amplitude $\bar{A}(\bar{B}^0 \rightarrow K^0\bar{K}^0)$ is given in Ref. [39],³ in which the QCD corrections are important for the hadronic matrix elements [41], as

$$\bar{A}(\bar{B}^0 \rightarrow K^0\bar{K}^0) \simeq \frac{4G_F}{\sqrt{2}} \sum_{q=u,c} V_{qb} V_{qd}^* [a_4^q(m_b) + r_\chi a_6^q(m_b)] X. \quad (30)$$

Here X is the factorized matrix element (see Ref. [39]) as

$$X = -if_K F_0(m_K^2)(m_B^2 - m_K^2), \quad (31)$$

where f_K and $F_0(m_K^2)$ denote the decay coupling constant of the K meson and the form factor, respectively, and $r_\chi = 2m_K^2/((m_b - m_s)(m_s + m_d))$ denotes the chiral enhancement factor. The coefficients a_i^q 's are given as [39,41]

³The $\bar{A}(\bar{B}^0 \rightarrow K^0\bar{K}^0)$ amplitude is explicitly presented in Refs. [39,41]. In our calculation, we neglect C_i ($i = 8-10$) since these Wilson coefficients are too small to contribute to the amplitude of $\bar{B}^0 \rightarrow K^0\bar{K}^0$ in our model.

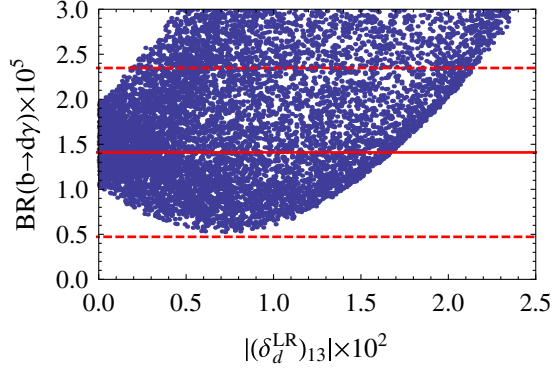


FIG. 6 (color online). The predicted region on the $|(\delta_d^{LR})_{13}|$ - $\text{BR}(b \rightarrow d\gamma)$ plane. The red solid and two red dotted lines denote the best fit value and upper and lower bounds of the experimental data with 90% C.L., respectively.

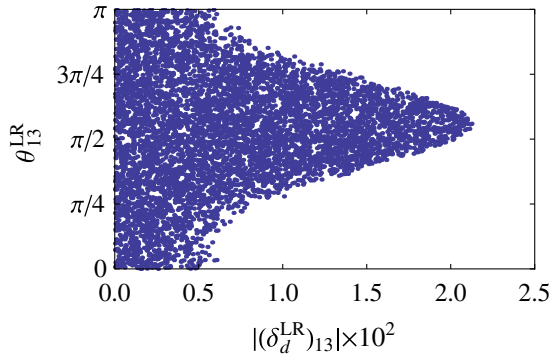


FIG. 7 (color online). The predicted region on the $(\delta_d^{LR})_{13}$ - θ_{13}^{LR} plane. The experimental constraint of $\text{BR}(b \rightarrow d\gamma)$ is taken into account.

$$\begin{aligned}
 a_4^q(m_b) &= (C_4 - \tilde{C}_4) + \frac{(C_3 - \tilde{C}_3)}{N_c} \\
 &+ \frac{\alpha_s(m_b)}{4\pi} \frac{C_F}{N_c} \left[(C_3 - \tilde{C}_3)[F_K + G_K(s_d) \right. \\
 &+ G_K(s_b)] + C_2 G_K(s_q) + [(C_4 - \tilde{C}_4) \\
 &+ (C_6 - \tilde{C}_6)] \sum_{f=u}^b G_K(s_f) + (C_{8G} - \tilde{C}_{8G}) G_{K,g} \Big], \\
 a_6^q(m_b) &= (C_6 - \tilde{C}_6) + \frac{(C_5 - \tilde{C}_5)}{N_c} \\
 &+ \frac{\alpha_s(m_b)}{4\pi} \frac{C_F}{N_c} \left[(C_3 - \tilde{C}_3)[G'_K(s_d) + G'_K(s_b)] \right. \\
 &+ C_2 G'_K(s_q) + [(C_4 - \tilde{C}_4) \\
 &+ (C_6 - \tilde{C}_6)] \sum_{f=u}^b G'_K(s_f) + (C_{8G} - \tilde{C}_{8G}) G'_{K,g} \Big],
 \end{aligned} \tag{32}$$

where q takes u and c quarks, $C_F = (N_c^2 - 1)/(2N_c)$, and the loop functions F_K , G_K , $G_{K,g}$, G'_K , and $G'_{K,g}$ are given in

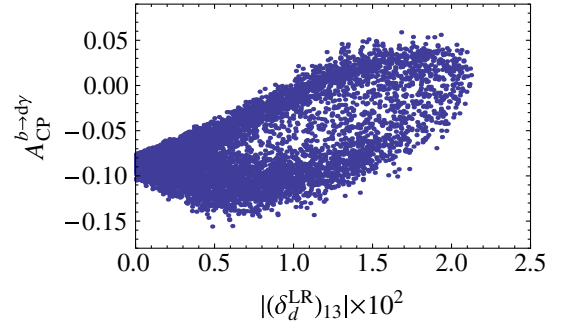


FIG. 8 (color online). The predicted direct CP asymmetry $A_{CP}^{b \rightarrow d\gamma}$ versus $|(\delta_d^{LR})_{13}|$.

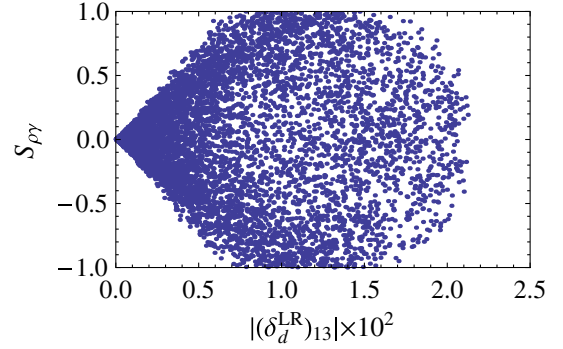


FIG. 9 (color online). The predicted time-dependent CP asymmetry $S_{\rho\gamma}$ versus $|(\delta_d^{LR})_{13}|$.

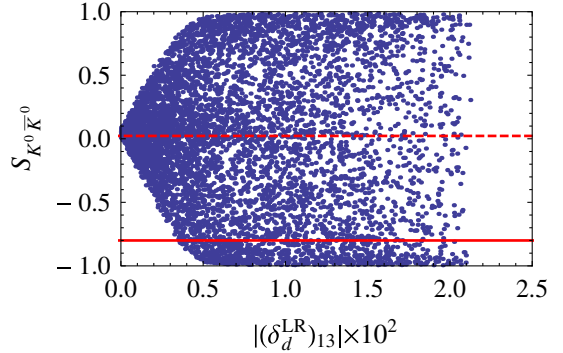


FIG. 10 (color online). The predicted time-dependent CP asymmetry $S_{K^0 \bar{K}^0}$ versus $|(\delta_d^{LR})_{13}|$. The red solid and red dotted lines denote the best fit value and the experimental data with 90% C.L., respectively.

Refs. [39,41]. The internal quark mass in the penguin diagrams enters as $s_f = m_f^2/m_b^2$.⁴ The minus sign in front of \tilde{C}_i ($i = 3-6, 8G$) comes from the parity of the final state as discussed in the previous section.

⁴The $C_i^{\tilde{g}}$ ($i = 3-6, 8G$) in Eq. (32) should be taken as the replacement $C_i^{\tilde{g}} \rightarrow [(V_{ib} V_{id}^*)/(V_{qb} V_{qd}^*)] C_i^q$ in Eq. (4).

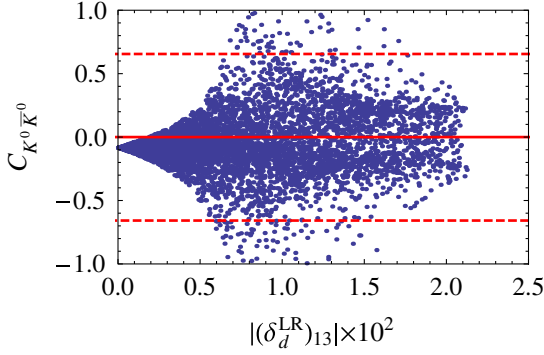


FIG. 11 (color online). The predicted time-dependent CP asymmetry $C_{K^0 \bar{K}^0}$ versus $|(\delta_d^{LR})_{13}|$. The red solid and two red dotted lines denote the best fit value and upper and lower bounds of the experimental data with 90% C.L., respectively.

By using the above formulations, we estimate the SUSY contributions in the $b \rightarrow d$ transition. In our calculations, we take $\mu \tan \beta$ to be 1 TeV, and we set the MI parameters $|(\delta_d^{LL})_{13}| = |(\delta_d^{LR})_{13}| \lesssim 10^{-2}$ from our previous works [7,8]. We also assume that the magnitudes of the MI parameters $(\delta_d^{LR})_{13}$ and $(\delta_d^{RL})_{13}$ are the same but each phase is different. Thus, we parameterize the MI parameters as follows:

$$(\delta_d^{LR})_{13} = |(\delta_d^{LR})_{13}| e^{2i\theta_{13}^{LR}}, \quad (\delta_d^{RL})_{13} = |(\delta_d^{LR})_{13}| e^{2i\theta_{13}^{RL}}. \quad (33)$$

Let us discuss the numerical analysis. In our calculations, we use the squark mass and the gluino mass as given in Eq. (22). The present experimental data of $\text{BR}(b \rightarrow d\gamma)$ in Eq. (25) gives a constraint for the MI parameters as seen in Fig. 6. The SM contribution is larger than the SUSY one until $|(\delta_d^{LR})_{13}| \simeq 7 \times 10^{-3}$, while the SUSY

contribution dominates the $b \rightarrow d\gamma$ decay in the region of $|(\delta_d^{LR})_{13}| \gtrsim 7 \times 10^{-3}$. It is remarked that there is a lower bound of the branching ratio around 5×10^{-6} .

In Fig. 7, we show the allowed region of $(\delta_d^{LR})_{13}$ within 90% C.L. of $\text{BR}(b \rightarrow d\gamma)$. It is found that any value of the phase is allowed in $|(\delta_d^{LR})_{13}| \lesssim 5 \times 10^{-3}$. The upper bound of the MI parameter is at $|(\delta_d^{LR})_{13}| \simeq 2 \times 10^{-2}$ around the specific θ_{13}^{LR} , $\pi/2$.

By using this allowed region of $(\delta_d^{LR})_{13}$, we can predict the direct CP asymmetry $A_{CP}^{b \rightarrow d\gamma}$ and time-dependent CP asymmetries $S_{\rho\gamma}$, $S_{K^0 \bar{K}^0}$, and $C_{K^0 \bar{K}^0}$. In Fig. 8, we show the predicted direct CP asymmetry $A_{CP}^{b \rightarrow d\gamma}$ versus $|(\delta_d^{LR})_{13}|$. Here the value at $|(\delta_d^{LR})_{13}| = 0$ is the SM one, $A_{CP}^{b \rightarrow d\gamma}(\text{SM}) \simeq -0.09$. Our prediction is $-0.16 \leq A_{CP}^{b \rightarrow d\gamma} \leq 0.06$. If $A_{CP}^{b \rightarrow d\gamma}$ is measured in the future, we will obtain an additional constraint of the MI parameters.

In Fig. 9, we show the prediction of $S_{\rho\gamma}$ depending on $|(\delta_d^{LR})_{13}|$. The SM prediction is $S_{\rho\gamma}(\text{SM}) \simeq (2m_d/m_b) \times \sin \phi_d \simeq 2.0 \times 10^{-3}$ [36], while the experimental data are $S_{\rho\gamma}(\text{exp}) = -0.8 \pm 0.7$ [22]. In our prediction, the $S_{\rho\gamma}$ reaches ± 1 at $|(\delta_d^{LR})_{13}| \gtrsim 7 \times 10^{-3}$. Therefore, the $S_{\rho\gamma}$ is expected to be much larger than the SM prediction in the case of $|(\delta_d^{LR})_{13}| = \mathcal{O}(10^{-3})$. We expect the precise data to test our prediction in the future.

In Figs. 10 and 11, we show the predictions of the time-dependent CP asymmetries $S_{K^0 \bar{K}^0}$ and $C_{K^0 \bar{K}^0}$ depending on $|(\delta_d^{LR})_{13}|$, respectively. In the SM, one predicts $0.02 \leq S_{K^0 \bar{K}^0}(\text{SM}) \leq 0.13$ and $-0.17 \leq C_{K^0 \bar{K}^0}(\text{SM}) \leq -0.15$ [39], while the experimental data are given as $S_{K^0 \bar{K}^0}(\text{exp}) = -0.8 \pm 0.5$ and $C_{K^0 \bar{K}^0}(\text{exp}) = 0.0 \pm 0.4$ [22], respectively. The present experimental bounds do not give any additional constraints to Fig. 7. However, more precise experimental data provide intensive constraints for MI parameters.

TABLE I. Summary of the SM predictions, experimental values, and our predictions.

	Exp.	SM	Our prediction
$\text{BR}(b \rightarrow s\gamma)$	$(3.53 \pm 0.24) \times 10^{-4}$ [22]	$(3.15 \pm 0.23) \times 10^{-4}$ [37]	Constraint
$\text{BR}(b \rightarrow d\gamma)$	$(1.41 \pm 0.57) \times 10^{-5}$ [24,25]	$(1.54^{+0.26}_{-0.31}) \times 10^{-5}$ [25]	Constraint
$A_{CP}^{b \rightarrow s\gamma}$	-0.008 ± 0.029 [22]	4×10^{-3} [35]	-0.03 – 0.03
$A_{CP}^{b \rightarrow d\gamma}$...	-0.09	-0.16 – 0.06
$S_{J/\psi K_S}$	0.679 ± 0.020 [23]	Input	Constraint
$S_{\phi K_S}$	$0.74^{+0.11}_{-0.13}$ [23]	$= S_{J/\psi K_S}$	Constraint
$S_{\eta' K^0}$	0.59 ± 0.07 [23]	$= S_{J/\psi K_S}$	Constraint
$\phi_s (S_{J/\psi \phi} = -\sin \phi_s)$	$-0.004 \pm 0.166 \pm 0.054$ [29]	$-0.0363^{+0.0016}_{-0.0015}$ [38]	Constraint
$S_{\phi \phi}$...	$= S_{J/\psi \phi}$	-0.2 – 0.4
$S_{\phi \eta'}$...	$= S_{J/\psi \phi}$	-0.5 – 0.4
$S_{K^e \gamma}$	-0.15 ± 0.22 [22]	0.04 [36]	-0.4 – 0.2
$S_{\rho\gamma}$	-0.8 ± 0.7 [22]	0.002 [36]	-1 – 1
$S_{K^0 \bar{K}^0}$	-0.8 ± 0.5 [22]	0.02 – 0.13 [39]	-1 – 1
$C_{K^0 \bar{K}^0}$	-0.0 ± 0.4 [22]	-0.17 to -0.15 [39]	-1 – 1

V. SUMMARY

We have discussed the contribution of the gluino-squark mediated flavor changing process to the CP violation in $b \rightarrow s$ and $b \rightarrow d$ transitions taking account of recent experimental data. We have presented the allowed region of the MI parameters $(\delta_d^{LR})_{23}$ and $(\delta_d^{LR})_{13}$, which are constrained by the branching ratios of $b \rightarrow s\gamma$ and $b \rightarrow d\gamma$ decays. In addition, the time-dependent CP asymmetries of $B^0 \rightarrow J/\psi K_S$, $B^0 \rightarrow \phi K_S$, and $B^0 \rightarrow \eta' K^0$ decays severely restrict the allowed region of the MI parameter, $(\delta_d^{LR})_{23}$. These MI parameters $(\delta_d^{LR})_{23}$ and $(\delta_d^{LR})_{13}$ are still allowed up to 2×10^{-2} for the squark and gluino masses of 1.5 TeV. If $m_{\tilde{q}} \approx m_{\tilde{g}}$ increase, the bound of $(\delta_d^{LR})_{k3}$ ($k = 2, 1$) is approximately rescaled as $(\delta_d^{LR})_{k3} \times m_{\tilde{q}}/(1.5 \text{ TeV})$.

By using these constraints, we predict the CP asymmetries of $B_s \rightarrow \phi\phi$, $B_s \rightarrow \eta'\phi$, and $B^0 \rightarrow K^0\bar{K}^0$ decays, as well as the CP asymmetries in $b \rightarrow s\gamma$ and $b \rightarrow d\gamma$ decays. We have summarized our results in Table I. It is remarked that the CP violation of the $B_s \rightarrow \phi\phi$ decay is expected to be large owing to the squark flavor mixing. This prediction will be tested soon at LHCb.

ACKNOWLEDGMENTS

We thank S. Mishima for useful discussions. We also thank A. Hayakawa and J. Kumagai for their help. M. T. is supported by JSPS Grand-in-Aid for Scientific Research, Grants No. 21340055 and No. 24654062.

-
- [1] G. Aad *et al.* (ATLAS Collaboration), *Phys. Lett. B* **716**, 1 (2012); S. Chatrchyan *et al.* (CMS Collaboration), *Phys. Lett. B* **716**, 30 (2012).
- [2] G. Aad *et al.* (ATLAS Collaboration), *Phys. Rev. D* **87**, 012008 (2013); S. Chatrchyan *et al.* (CMS Collaboration), *Phys. Lett. B* **713**, 408 (2012).
- [3] A. Bharucha *et al.* (LHCb Collaboration), [arXiv:1208.3355](https://arxiv.org/abs/1208.3355).
- [4] R. Aaij *et al.* (LHCb Collaboration), *Phys. Rev. Lett.* **110**, 021801 (2013).
- [5] D. Lambert (LHCb Collaboration), [arXiv:1206.3188](https://arxiv.org/abs/1206.3188).
- [6] M. Kobayashi and T. Maskawa, *Prog. Theor. Phys.* **49**, 652 (1973).
- [7] A. Hayakawa, Y. Shimizu, M. Tanimoto, and K. Yamamoto, *Phys. Lett. B* **710**, 446 (2012).
- [8] Y. Shimizu, M. Tanimoto, and K. Yamamoto, *Prog. Theor. Phys.* **128**, 273 (2012).
- [9] S. F. King, *J. High Energy Phys.* **09** (2010) 114.
- [10] M. Endo, S. Shirai, and T. T. Yanagida, *Prog. Theor. Phys.* **125**, 921 (2011).
- [11] M. Endo and N. Yokozaki, *J. High Energy Phys.* **03** (2011) 130.
- [12] J. Kubo and A. Lenz, *Phys. Rev. D* **82**, 075001 (2010).
- [13] Y. Kaburaki, K. Konya, J. Kubo, and A. Lenz, *Phys. Rev. D* **84**, 016007 (2011).
- [14] J. K. Parry, *Phys. Lett. B* **694**, 363 (2011).
- [15] P. Ko and J.-h. Park, *Phys. Rev. D* **80**, 035019 (2009).
- [16] P. Ko and J.-h. Park, *Phys. Rev. D* **82**, 117701 (2010).
- [17] R.-M. Wang, Y.-G. Xu, Q. Chang, and Y.-D. Yang, *Phys. Rev. D* **83**, 095010 (2011).
- [18] A. Crivellin and U. Nierste, *Phys. Rev. D* **79**, 035018 (2009).
- [19] L. Hofer, U. Nierste, and D. Scherer, *J. High Energy Phys.* **10** (2009) 081.
- [20] A. Crivellin, L. Hofer, and J. Rosiek, *J. High Energy Phys.* **07** (2011) 017.
- [21] H. Ishimori, Y. Kajiyama, Y. Shimizu, and M. Tanimoto, *Prog. Theor. Phys.* **126**, 703 (2011).
- [22] J. Beringer *et al.* (Particle Data Group Collaboration), *Phys. Rev. D* **86**, 010001 (2012).
- [23] Y. Amhis *et al.* (Heavy Flavor Averaging Group Collaboration), [arXiv:1207.1158](https://arxiv.org/abs/1207.1158).
- [24] P. del Amo Sanchez *et al.* (BABAR Collaboration), *Phys. Rev. D* **82**, 051101 (2010).
- [25] A. Crivellin and L. Mercolli, *Phys. Rev. D* **84**, 114005 (2011).
- [26] G. Buchalla, A. J. Buras, and M. E. Lautenbacher, *Rev. Mod. Phys.* **68**, 1125 (1996).
- [27] M. Endo and S. Mishima, [arXiv:hep-ph/0408138](https://arxiv.org/abs/hep-ph/0408138).
- [28] T. Aushev *et al.*, [arXiv:1002.5012](https://arxiv.org/abs/1002.5012).
- [29] S. Stone (LHCb Collaboration), in Proceedings of ICHEP 2012 (unpublished).
- [30] M. Endo, S. Mishima, and M. Yamaguchi, *Phys. Lett. B* **609**, 95 (2005).
- [31] S. Khalil and E. Kou, *Phys. Rev. Lett.* **91**, 241602 (2003).
- [32] R. Harnik, D. T. Larson, H. Murayama, and A. Pierce, *Phys. Rev. D* **69**, 094024 (2004).
- [33] S. Mishima and A. I. Sanda, *Prog. Theor. Phys.* **110**, 549 (2003).
- [34] A. J. Buras, [arXiv:hep-ph/9806471](https://arxiv.org/abs/hep-ph/9806471).
- [35] A. L. Kagan and M. Neubert, *Phys. Rev. D* **58**, 094012 (1998).
- [36] D. Atwood, M. Gronau, and A. Soni, *Phys. Rev. Lett.* **79**, 185 (1997).
- [37] M. Misiak *et al.*, *Phys. Rev. Lett.* **98**, 022002 (2007).
- [38] J. Charles *et al.*, *Phys. Rev. D* **84**, 033005 (2011).
- [39] A. K. Giri and R. Mohanta, *J. High Energy Phys.* **11** (2004) 084.
- [40] R. Fleischer and S. Recksiegel, *Eur. Phys. J. C* **38**, 251 (2004).
- [41] T. Muta, A. Sugamoto, M.-Z. Yang, and Y.-D. Yang, *Phys. Rev. D* **62**, 094020 (2000).